Journal of Magnetic Resonance 200 (2009) 88–94

Contents lists available at ScienceDirect

Journal of Magnetic Resonance

journal homepage: www.elsevier.com/locate/jmr

Quantitative analysis of Earth's field NMR spectra of strongly-coupled heteronuclear systems

Meghan E. Halse [a], Paul T. Callaghan [a,*], Brett C. Feland [b], Roderick E. Wasylishen [b,*]

[a] MacDiarmid Institute for Advanced Materials and Nanotechnology, School of Chemical and Physical Sciences, Victoria University of Wellington, Post Office Box 600, Wellington 6012, New Zealand
[b] Department of Chemistry, University of Alberta, E3-24 Chemistry Centre, Edmonton, Alta., Canada T6G 2G2

ARTICLE INFO

Article history:
Received 29 May 2009
Available online 18 June 2009

Keywords:
Earth's magnetic field
Perturbation theory
Heteronuclear indirect spin–spin coupling
Strong coupling
NMR
Spectroscopy

ABSTRACT

In the Earth's magnetic field, it is possible to observe spin systems consisting of unlike spins that exhibit strongly coupled second-order NMR spectra. Such spectra result when the *J*-coupling between two unlike spins is of the same order of magnitude as the difference in their Larmor precession frequencies. Although the analysis of second-order spectra involving only spin-½ nuclei has been discussed since the early days of NMR spectroscopy, NMR spectra involving spin-½ nuclei and quadrupolar ($I > ½$) nuclei have rarely been treated. Two examples are presented here, the tetrahydroborate anion, BH_4^-, and the ammonium cation, NH_4^+. For the tetrahydroborate anion, $^1J(^{11}B,^1H) = 80.9$ Hz, and in an Earth's field of 53.3 μT, $\nu(^1H) = 2269$ Hz and $\nu(^{11}B) = 728$ Hz. The ^1H NMR spectra exhibit features that both first- and second-order perturbation theory are unable to reproduce. On the other hand, second-order perturbation theory adequately describes ^1H NMR spectra of the ammonium anion, $^{14}NH_4^+$, where $^1J(^{14}N,^1H) = 52.75$ Hz when $\nu(^1H) = 2269$ Hz and $\nu(^{14}N) = 164$ Hz. Contrary to an early report, we find that the ^1H NMR spectra are independent of the sign of $^1J(^{14}N,^1H)$. Exact analysis of two-spin systems consisting of quadrupolar nuclei and spin-½ nuclei are also discussed.

1. Introduction

Pioneering Earth's field NMR (EFNMR) experiments were conducted by several research groups in the 1950s and 1960s [1–9]. Recently, renewed interest in EFNMR has resulted from the development of inexpensive pulse-FT spectrometers that are ideally suited for introducing students to the fundamentals of nuclear magnetic resonance spectroscopy – spectral acquisitions, NMR relaxation and spectral analysis. The advent of innovative signal detection schemes, such as the use of super-conducting quantum interference devices (SQUIDs) or atomic magnetometers for detecting nuclear precession in microtesla fields [10–15], have also added to the increased interest in NMR spectroscopy and imaging at (or below) the Earth's magnetic field.

EFNMR spectroscopy is made possible, in part, by the homogeneity of the Earth's field which allows for absolute spectral resolution comparable or, in some cases, superior to those achieved using modern super-conducting magnets [16,17]. However, in contrast to super-conducting magnets, the Earth's field is homogeneous over sample sizes on the order of half a liter and so the weak nature of this field can be partly obviated by the use of large samples.

The purpose of this article is to discuss some of the subtleties of analyzing Earth's field NMR spectra. While analysis of complex spin-½ NMR spectra has been well developed for many years [18], analysis of tightly coupled spin systems where one spin is a quadrupolar nucleus ($I > ½$) while the other nuclei in the spin system are spin-½ has not previously been discussed. Herein we present two examples of such spin systems and demonstrate the efficacy of perturbation theory for modeling and understanding these systems. As well, we discuss the requirements for determining the signs of indirect spin–spin coupling constants in Earth's field NMR experiments.

2. Theory

2.1. Analysis of strong indirect spin–spin coupling in Earth's field NMR

One of the distinguishing features of ^1H NMR spectroscopy carried out in the relatively weak Earth's magnetic field ($B_E \sim 0.5$ G or 50 μT) is the observation of strong indirect spin–spin coupling between heteronuclei. While the NMR spectra of tightly coupled nuclei of the same species, so-called AB spectra, are commonly observed using high-field laboratory NMR spectrometers, the dif-

* Corresponding authors. Fax: +64 4 463 5237 (P.T. Callaghan), +1 780 492 8231 (R.E. Wasylishen).
E-mail addresses: Paul.Callaghan@vuw.ac.nz (P.T. Callaghan), roderick.wasylishen@ualberta.ca (R.E. Wasylishen).

1090-7807/$ - see front matter © 2009 Elsevier Inc. All rights reserved.
doi:10.1016/j.jmr.2009.06.012

ference in Larmor frequency between heteronuclei in super-conducting magnets is such that the weak coupling condition is always satisfied for spin systems. Therefore, working in the Earth's magnetic field provides a unique opportunity to observe and analyze the spectra of tightly coupled nuclei of differing spin.

2.1.1. Perturbation theory

In 1956, W.A. Anderson used perturbation theory to derive expressions which could be used to predict the form of tightly coupled NMR spectra for systems of chemically non-equivalent spins [19]. A pedagogical overview of the analysis of tightly coupled NMR spectra using perturbation theory was presented by E.W. Garbisch in 1968 [20–22]. Further detailed discussions of the applications of perturbation theory in NMR can be found in the classic text by P.L. Corio [23].

Following the standard procedure for time-independent perturbation theory, the full Hamiltonian is re-expressed in terms of an unperturbed part, $\mathscr{H}_\mathbf{0}$, and a perturbation, $\mathscr{H}_\mathbf{1}$, where λ is a dimensionless quantity which takes a value between 0 and 1.

$$\mathscr{H} = \mathscr{H}_\mathbf{0} + \lambda\mathscr{H}_\mathbf{1} \tag{1}$$

In the approach of Anderson the unperturbed Hamiltonian, $\mathscr{H}_\mathbf{0}$, is taken to be the Zeeman Hamiltonian, as shown in Eq. (2), where γ is the magnetogyric ratio. Note that in this paper we express all Hamiltonians in units of angular frequency.

$$\mathscr{H}_\mathbf{0} = -\sum_R \gamma_R B_E \mathbf{I}_{zR} \tag{2}$$

The summation in Eq. (2) is performed over all of the groups of magnetically equivalent nuclei within the spin system. Note that $\mathbf{I}_R$ is the total angular momentum operator resulting from the vector coupling of the spins within the group denoted by the subscript R. Therefore $\mathbf{I}_{zR}$ is the vector sum of the z components of the angular momentum operators for each of the N_R magnetically equivalent R group spins.

$$\mathbf{I}_{zR} = \sum_{S=1}^{N_R} \mathbf{I}_{zS}$$

The unperturbed eigenfunctions are written as the product of the individual kets, $|I_R m_R\rangle$, for each group of magnetically equivalent spins using the product operator formalism.

No chemical shift term is included in Eq. (2) because, except in a few unusual cases [24], chemical shifts are vanishingly small in the Earth's field. Also it is important to note that this approach does not take into account the possibility of chemically equivalent but magnetically non-equivalent nuclei and therefore, in the Earth's magnetic field, this approach only applies to heteronuclear indirect spin–spin coupling. To include the effects of chemically equivalent but magnetically non-equivalent nuclei, the secular terms of the indirect spin–spin coupling Hamiltonian must be included in the unperturbed Hamiltonian as demonstrated by Hecht [25].

The perturbation, $\mathscr{H}_\mathbf{1}$, is given by the Hamiltonian for heteronuclear indirect spin–spin coupling (Eq. (3)), where J_{RS} is the coupling constant, in frequency units, between the R and S groups of magnetically equivalent spins.

$$\begin{aligned}\mathscr{H}_\mathbf{1} &= \sum_R \sum_{S>R} 2\pi J_{RS} \mathbf{I}_R \cdot \mathbf{I}_S \\ &= \sum_R \sum_{S>R} 2\pi J_{RS} \left\{ \mathbf{I}_{zR}\mathbf{I}_{zS} + \frac{1}{2}\left(\mathbf{I}_R^+ \mathbf{I}_S^- + \mathbf{I}_R^- \mathbf{I}_S^+\right)\right\}\end{aligned} \tag{3}$$

Notice that Eq. (3) differs from the corresponding expression of Anderson [19] by our inclusion of the $\mathbf{I}_R^- \mathbf{I}_S^+$ term and the ½ factor.

In Appendix II of Ref. [19] Anderson derived expressions for the first-, second- and third-order perturbation energies. However, we found that Anderson's expression for the third-order term is inconsistent with spectra calculated numerically using density matrix theory. In Eq. (4) we present terms for the perturbation energies (in angular frequency units) which we have derived up to third-order.

$$E^0(I_A, m_A, I_B, m_B \ldots) = -\sum_R \omega_R m_R$$

$$E^{(1)}(I_A, m_A, I_B, m_B \ldots) = 2\pi \sum_R \sum_{S>R} J_{RS} m_R m_S$$

$$E^{(2)}(I_A, m_A, I_B, m_B \ldots) = -4\pi^2 \sum_R \sum_{S>R} \frac{J_{RS}^2}{2(\omega_R - \omega_S)} \left[m_R\left(I_S^2 + I_S - m_S^2\right) - m_S\left(I_R^2 + I_R - m_R^2\right)\right]$$

$$\begin{aligned}E^{(3)}(I_A, m_A, I_B, m_B \ldots) &= -8\pi^3 \sum_R \sum_{S>R} \frac{J_{RS}^3}{2(\omega_R - \omega_S)^2} [F(R)F(S) \\ &+ F(R)m_S(1 - m_S + m_R) + F(S)m_R(1 - m_R + m_S)] \\ &+ 8\pi^3 \sum_R \sum_{S>R} \sum_{T>S} \frac{J_{RS} J_{RT} J_{ST}}{(\omega_R - \omega_S)(\omega_R - \omega_T)(\omega_S - \omega_T)} \\ &\times \begin{bmatrix} m_S m_T F(R)(\omega_S - \omega_T) \\ -m_R m_T F(S)(\omega_R - \omega_T) \\ +m_R m_S F(T)(\omega_R - \omega_S) \end{bmatrix}\end{aligned} \tag{4}$$

where

$$\omega_R = \gamma_R B_E$$
$$F(R) = I_R(I_R + 1) - m_R(m_R + 1)$$

Note that the energy terms in Eq. (4) are calculated for an arbitrary number of groups of magnetically equivalent heteronuclei and the summations over R, S, and, in the case of the third-order energy, T, are carried out such that the coupling between two groups of spins is only counted once.

For the spectra calculated using perturbation theory in this paper, the transition probabilities for the various ^{1}H transitions were not explicitly calculated. When comparing observed and calculated spectra, we consider only peak frequencies, not peak integrals or heights. Calculations of transition probabilities can be found elsewhere [23,25,26].

2.1.2. Comparison of perturbation theory and exact calculations

In this paper we consider the case of a group of spin-½ nuclei (e.g., four ^{1}H's) coupled to a quadrupolar nucleus such as ^{14}N ($I = 1$), ^{10}B ($I = 3$) or ^{11}B ($I = 3/2$). In order to determine the validity of the perturbation theory approach to modeling this problem we first consider a simple two-spin case, which can be solved exactly through diagonalization of the full Hamiltonian [18,23,27], and compare the resultant exact transition frequencies with those given by first-, second- and third-order perturbation theory.

The results for the case of a single ^{1}H coupled to a single ^{11}B in the Earth's magnetic field of 54 μT are presented in Fig. 1. The difference between the exact ^{1}H transition frequencies (of which there are four in this case) and the transition frequencies calculated from first-order (short dashed line), second-order (long dashed line) and third-order (solid line) perturbation theory is shown as a function of the indirect spin–spin coupling constant between the $I = 1/2$ and $I = 3/2$ nuclei. Note that two of the first-order transition frequencies coincide and so only three first-order transitions are apparent. In addition, one of the second-order transition frequencies is exactly equal to one of the third-order transition frequencies and so is entirely obscured. ^1J

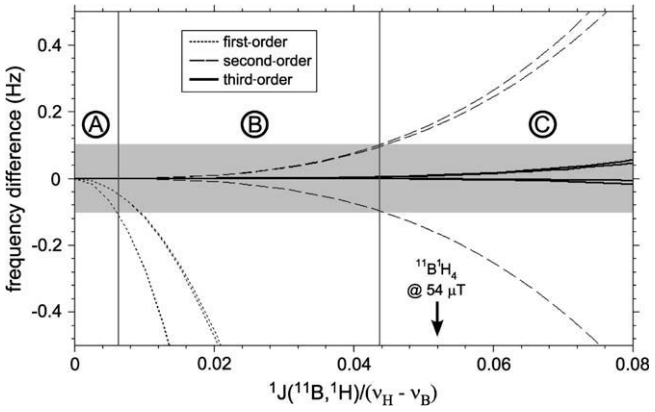

Fig. 1. The difference between the exact ^{1}H transition frequencies and those predicted by first-order (short dashed line) second-order (long dashed line) and third-order (solid line) perturbation theory as a function of the relative strength of the indirect spin–spin coupling constant for a single ^{1}H nucleus coupled to a single ^{11}B nucleus in a field of 54 μT. The indirect spin–spin coupling constant is expressed as a fraction of the difference in Larmor frequency between the ^{1}H (2299 Hz) and ^{11}B (738 Hz) nuclei. The shaded area highlights the range of unobservable frequency differences which are less than the target resolution of the experiment (0.1 Hz). Using this target resolution as a guide, the plot is divided into the regions A, B and C in which first-, second- and third-order perturbation theory (respectively) can be used to accurately model the spin system. The indirect spin–spin coupling constant $^1J(^1H,^{11}B)$ = 80.9 Hz of $NaBH_4$ falls within the third-order region in a field of 54 μT.

(^{1}H,^{11}B) is expressed as a fraction of the difference between the Larmor frequency of the protons (2299 Hz) and that of the ^{11}B nucleus (738 Hz) at 54 μT. The shaded area in Fig. 1 indicates the range of frequency differences which are unobservable in an experimental spectrum, assuming an experimental resolution of 0.1 Hz. Using this region as a guide, we can define values of J for which (A) first-order, (B) second-order, and (C) third-order perturbation theory accurately models the observed spectrum. These regions are labeled accordingly in Fig. 1.

For the $NaBH_4$ sample examined in the experimental portion of this paper, the indirect spin–spin coupling constant between ^{11}B and ^{1}H (80.9 Hz) is approximately 5.2% of the difference in Larmor frequency between ^{11}B and ^{1}H nuclei in a field of 54 μT. Therefore it is expected that this spectrum will be well characterized by third-order perturbation theory.

While the two-spin example is informative, it does not fully illustrate the effect of the second- and third-order energy contributions for an AB_n spectrum where $n > 1$ and A is a quadrupolar ($I > ½$) nucleus. Due to the complexity involved in obtaining closed form analytical solutions to the Schrödinger equation for large spin systems under the influence of strong indirect spin–spin coupling, we use numerical simulations to calculate the exact spectra for the case of more than two spins and compare these results with perturbation theory.

Exact spectra of strongly coupled spin systems in the Earth's magnetic field can be numerically simulated using a number of mathematical tools. In this paper we use a density matrix and product operator approach [26,28–30]. The density matrix formalism provides a convenient way to describe the statistical state of the coupled spin system and to evolve this system as a function of time under the influence of the full interaction Hamiltonian.

We start the numerical simulation, at time $t = 0$, with the density matrix at thermal equilibrium, $\boldsymbol{\rho}(0)$. We can numerically simulate the excitation pulse through the use of a rotation operator about x, $\mathbf{R}_x(\theta)$. $\mathbf{R}_x(\theta)$ is a product operator which only acts on the spins in the system that we wish to excite, i.e., the ^{1}H nuclei. Following the excitation pulse, the system is allowed to evolve with time according to an evolution operator, $\mathbf{U}(t)$, where the full interaction Hamiltonian, $\mathscr{H}$, is the sum of $\mathscr{H}_\mathbf{0}$ (Eq. (2)) and $\mathscr{H}_\mathbf{1}$ (Eq. (3)). Indirect spin–spin coupling in the Earth's magnetic field does not, in general, satisfy the weak coupling condition and so the full Hamiltonian, not just the secular terms, must be used. The evolution operator is evaluated as a Taylor expansion calculated to a fixed order, O (Eq. (5)).

$$\mathbf{U}(\Delta t) \approx \sum_{n=0}^{O} \frac{(-1)^n i^n}{n!} \mathscr{H}^n \Delta t^n = \mathbf{1} - i\mathscr{H}\Delta t - \frac{1}{2}\mathscr{H}\mathscr{H}\Delta t^2 + \ldots \tag{5}$$

The evolution time step, Δt, and the order of the Taylor expansion, O, in Eq. (5) must be chosen such that the error associated with the truncation of the Taylor Series is much less than 1. The dimensionless error for a single application of the evolution operator is on the order of $\frac{(\Delta\omega\Delta t)^O}{O!}$, where $\Delta\omega$ is the bandwidth, in angular frequency, of the calculated spectrum. This error is additive with each application of the evolution operator and so over the course of the simulation the cumulative error becomes $Err \approx 2\pi N_{pts}\frac{(\Delta\omega\Delta t)^{O-1}}{O!}$, where N_{pts} is the total number of spectral points spanning $\Delta\omega$. For the numerically simulated NMR spectra presented in this paper an order of $O = 28$ and evolution time steps on the order of a hundred μs were used to simulate spectra with $N_{pts} = 32{,}768$. This gives rise to an error of 10^{-11}. The evolution operator is calculated only once at the start of the numerical simulation and so using a large value of O does not carry a significant computational time penalty.

As the system evolves, we need to periodically observe the NMR signal at a fixed sampling time, Δt_2. Δt_2 can take any value which is an integer multiple of the evolution time Δt. The density matrix at $t = \Delta t_2$ is defined by Eq. (6), where $\boldsymbol{\rho}(0^+)$ denotes the density matrix immediately following the excitation pulse and the evolution operator, $\mathbf{U}(\Delta t)$ is applied m times, where $m = \frac{\Delta t_2}{\Delta t}$.

$$\boldsymbol{\rho}(\Delta t_2) = \mathbf{U}(\Delta t)\ldots\mathbf{U}(\Delta t)\boldsymbol{\rho}(0^+)\mathbf{U}^\dagger(\Delta t)\ldots\mathbf{U}^\dagger(\Delta t) \tag{6}$$

Observation of the system is achieved through the use of an observation operator as illustrated in Eq. (7).

$$S(\Delta t_2) = \overline{\langle \mathbf{I}_{obs} \rangle} = Tr(\mathbf{I}_{obs}\boldsymbol{\rho}(\Delta t_2)) \tag{7}$$

The observation operator for the detection of nuclear precession in NMR is defined by Eq. (8), where the sum is evaluated for each of the N observed nuclei in the system.

$$\mathbf{I}_{obs} = \sum_{n=1}^{N}(\mathbf{I}_{xn} + i\mathbf{I}_{yn}) \tag{8}$$

In Fig. 2 we present ^{1}H NMR spectra calculated from perturbation theory and using a density matrix numerical simulation for $^{11}B^1H_4^-$ acquired in a field of 54 μT with an indirect spin–spin coupling constant of $^1J(^{11}B,^1H) = 80.3$ Hz. The spectrum calculated from first-order perturbation theory (Fig. 2a) contains four lines, separated by $^1J(^{11}B,^1H)$, which correspond to the four spin states of the ^{11}B nucleus ($m = +3/2, +1/2, -1/2$ and $-3/2$). This is the form of the ^{1}H NMR spectrum of $^{11}B^1H_4^-$ in the high-field case, where the spins are weakly coupled and so the presence of a plurality of magnetically equivalent protons has no observed effect on the spectrum.

In the case of second-order perturbation theory (Fig. 2b) the complexity of the calculated spectrum is dramatically increased, with each of the four first-order peaks further split into quartets. It is also interesting to note that in the spectrum calculated with second-order perturbation theory the four multiplets are shifted to a slightly higher frequency, relative to the first-order perturbation theory peaks, and are no longer equally spaced. The additional peak multiplicity is due to the presence of the four magnetically equivalent protons coupled to the ^{11}B nucleus. This multiplicity in tightly coupled heteronuclear systems has previously been ob-

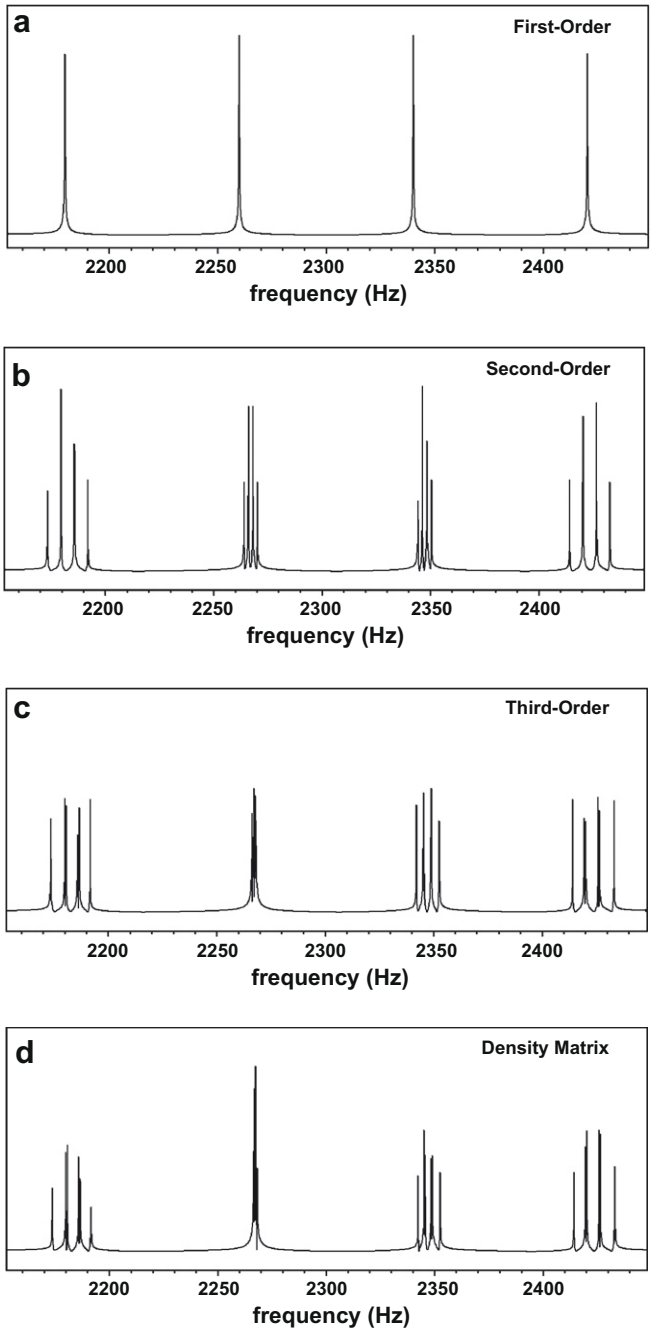

Fig. 2. Calculated ^{1}H NMR spectra of $^{11}B^{1}H_4^-$ in a field of 54 μT with $^{1}J(^{11}B,^{1}H) = 80.3$ Hz using: (a) first-order perturbation theory, (b) second-order perturbation theory, (c) third-order perturbation theory and (d) a numerical simulation based on density matrix theory.

served in the Earth's magnetic field in strongly coupled ^{13}C–^{1}H systems [31].

Second-order perturbation theory does not capture the full 6-fold multiplicity predicted for this system by the vector model of Appelt et al. [32]. According to this model, if we consider one of the four protons as the observed proton, the expected multiplicity is explained by the total angular momentum states of the remaining three protons. The total angular momentum quantum number of these spins can have a value of $I = 3/2$ or $I = 1/2$ with corresponding azimuthal quantum numbers of $m = 3/2, 1/2, -1/2, -3/2$ and $m = 1/2, -1/2$. To second-order the states: $I = 3/2$, $m = 1/2$ and $I = 1/2$, $m = 1/2$ as well as the states: $I = 3/2$, $m = -1/2$ and $I = 1/2$, $m = -1/2$ are degenerate and so only four lines are observed instead of the full six.

In the spectrum calculated using third-order perturbation theory (Fig. 2c) the full 6-fold multiplicity of the four sets of multiples is observed. The most striking feature of this spectrum is the strong asymmetry associated with this splitting of these multiplets. In this tightly coupled regime, the second multiplet collapses to what would, at a resolution of 0.5 Hz, appear to be a singlet. In the perturbation theory calculation there are six distinct transition frequencies associated with this multiplet but the splitting is very small and difficult to observe at the resolution (0.16 Hz) of the calculated spectrum.

Comparison of the calculated perturbation theory spectra (Fig. 2a–c) with the spectrum calculated using a density matrix simulation (Fig. 2d) illustrates, definitively, that a third-order perturbation theory calculation is necessary to accurately model this system. A fourth-order term was calculated and compared with the density matrix simulation. While the transition frequencies calculated from fourth-order perturbation theory provide better agreement with those of the density matrix simulation, the fourth-order contribution is very small and no significant difference in the overall characteristics of the spectrum is observed between third- and fourth-order. Therefore we conclude that, in this case, the addition of the fourth-order term is not particularly informative.

2.2. Determining the sign of indirect spin–spin coupling constants in EFNMR

At the Colloque Ampère XIV in 1967, Georges-J. Béné showed a portion of a frequency domain ^{1}H NMR spectrum of NH_4NO_3 acquired in the Earth's magnetic field and suggested that with improved resolution one could deduce the sign of $^{1}J(^{14}N,^{1}H)$ based on corrections to frequencies calculated using third-order perturbation theory [2]. However, numerical simulations of the ^{1}H NMR spectrum of a strongly coupled $^{14}N^{1}H_4^+$ spin system in the Earth's magnetic field using density matrix theory show that the form of this spectrum is independent of the absolute sign of $^{1}J(^{14}N,^{1}H)$.

We believe that this misconception came about because of an unfortunate error in Anderson's original expression for the third-order perturbation energy (Appendix II in Ref. [19]). NMR spectra calculated from this third-order energy term exhibit spectral features which are dependent on the absolute sign of ^{1}J(A,B) for strongly coupled AB_n systems, where $n > 1$, A is a quadrupolar ($I > ½$) nucleus and B is the observed spin-½ nucleus. For example, in the case of the $^{11}B^{1}H_4^-$ system discussed above, the asymmetry of the splitting of the four multiplets depends on the sign of J if the spectrum is calculated using Anderson's expression for the third-order perturbation energy. However, density matrix simulations show that the form of this spectrum is independent of the sign of J and ^{1}H EFNMR spectra of this system calculated using the third-order perturbation energy terms presented in Eq. (4) are also independent of the sign of J. Indeed we find that third-order perturbation theory, or for that matter exact analysis, will not yield the sign of any indirect spin–spin coupling constant in an A_mB_n spin system regardless of the spin of nucleus "A" and nucleus "B".

This is further illustrated by considering the exact expressions for the transition frequencies of the coupled two-spin ($^{11}B^{1}H$) system considered in Fig. 1. Closed form expressions for the four allowed ^{1}H transitions of this system are presented in Eq. (9), where ν_B and ν_H are the Larmor frequencies of the ^{11}B and ^{1}H nuclei, respectively.

$$T_1 = \frac{1}{2}\nu_B + \frac{1}{2}\nu_H + J + \frac{1}{2}\sqrt{(\nu_H - \nu_B)^2 + 2J(\nu_H - \nu_B) + 4J^2}$$
$$T_2 = \frac{1}{2}\nu_B + \frac{1}{2}\nu_H - J + \frac{1}{2}\sqrt{(\nu_H - \nu_B)^2 - 2J(\nu_H - \nu_B) + 4J^2}$$
$$T_3 = \nu_B + \frac{1}{2}\sqrt{(\nu_H - \nu_B)^2 + 4J^2} + \frac{1}{2}\sqrt{(\nu_H - \nu_B)^2 - 2J(\nu_H - \nu_B) + 4J^2}$$
$$T_4 = \nu_B + \frac{1}{2}\sqrt{(\nu_H - \nu_B)^2 + 4J^2} + \frac{1}{2}\sqrt{(\nu_H - \nu_B)^2 + 2J(\nu_H - \nu_B) + 4J^2} \quad (9)$$

Inspection of Eq. (9) shows that $T_1(-J) = T_2(J)$ and $T_3(-J) = T_4(J)$. Therefore a change in the sign of J will have no observable effect on the spectrum regardless of the relative strength of J and $(\nu_H - \nu_B)$.

A theorem which states that the NMR spectrum of any two spins, A and B, coupled via an indirect spin–spin coupling constant, $^1J(A,B)$, is invariant under the transformation $^1J(A,B) \rightarrow -^1J(A,B)$ is proved by P.L. Corio in his book on high resolution NMR spectra published in 1967 [23]. The absolute sign of J between two coupled spins can be determined using NMR if the two coupled spins are subject to additional interactions, such as weak residual dipolar coupling in an aligned medium [33].

The relative signs of J in tightly coupled systems of more than two groups of nuclei can be determined through comparison of observed and calculated EFNMR spectra. This application was discussed by Béné in his review of EFNMR in 1980 [34].

3. Results and discussion

Consider the ^{1}H NMR spectrum of an aqueous solution of ammonium nitrate. In the Earth's magnetic field, this spin system is an AB_4 spin system where $A = {}^{14}$N with a nuclear spin $I = 1$ and the B spins are four magnetically equivalent ^{1}H nuclei. In this case the natural abundance of ^{14}N and ^{1}H (99.6% and 99.9%, respectively) is such that no other isotopes of N and H need to be considered. This particular spin system was first investigated in the Earth's field by Brown and Thompson [6] who analyzed the free-induction decay and compared the observed frequency components with the spectrum calculated using second-order perturbation theory. The indirect spin–spin coupling of $^{14}N^1H_4^+$ was studied at high-field by Wasylishen and Friedrich in 1983 [35].

Fig. 3 presents a ^{1}H EFNMR spectrum acquired for a 500 mL aqueous solution of 8 M NH_4NO_3 and 2 M HCl. This spectrum was acquired using 49 scans in a total experiment time of 12 min. Below the experimental spectrum is a ^{1}H NMR spectrum calculated using second-order perturbation theory with $^1J(^{14}N,^1H) = 52.75$ Hz, $B_E = 53.3$ μT and a line broadening of 0.16 Hz. In this case $^1J(^{14}N,^1H)$ is 2.5% of the difference in Larmor frequency between ^{14}N and ^{1}H (2105 Hz). A portion of a ^{1}H NMR spectrum of NH_4NO_3 acquired in the Earth's magnetic field was previously presented, in 1967, by Georges-J. Béné [2]. The spectrum presented in Fig. 3 is of comparable quality to this previously reported result.

By inspection, we see that the features of the ^{1}H NMR spectrum of the ammonium ion are well characterized by second-order perturbation theory. The central peak is split into a dominant component at 2269.5 Hz, which corresponds to the solvent protons, and a weaker component, shifted to slightly higher frequency, which corresponds to the spin state $m = 0$ of the ^{14}N nucleus in the $^{14}N^1H_4^+$ ion. The two multiplets, which correspond to the $m = \pm 1$ spin states of the ^{14}N nucleus, consist of four peaks and are not symmetric about the central peak but rather are shifted to slightly higher frequencies relative to the expected first-order peak positions of $\nu_H \pm J$, where ν_H is the proton Larmor frequency.

Now we consider the case of the BH_4^- anion, studied previously at high-field by Smith et al. [36]. An experimental ^{1}H Earth's Field NMR spectrum of the borohydride anion in an aqueous solution of sodium borohydride and sodium hydroxide is presented in Fig. 4. In this case we focus our attention on two different species: $^{11}BH_4^-$ where ^{11}B has a nuclear spin of $I = 3/2$ and a natural abundance of approximately 80% and $^{10}BH_4^-$ where ^{10}B has a nuclear spin of $I = 3$ and a natural abundance of approximately 20%. Prior to taking the magnitude of the spectrum in Fig. 4, a complex Lorentzian line, centered about 2269.4 Hz and with a 1.1 Hz linewidth, was subtracted from the complex experimental spectrum to suppress the dominant peak corresponding to the solvent protons so that all of the BH_4^- multiplets could be easily identified in the magnitude spectrum. The central peak in the resultant spectrum is the unsuppressed portion of this solvent proton peak. Due to imperfections in the B_1 transceiver coil, the spectrum could not be correctly phased over the full bandwidth. Portions of the real spectrum, which have been phased locally, are shown in the insets to Fig. 4 to illustrate the spectral resolution available in the complex spectrum.

Below the experimental spectrum of the tetrahydroborate ion is a the spectrum calculated from third-order perturbation theory with $^1J(^{11}B,^1H) = 80.9$ Hz, $^1J(^{10}B,^1H) = 27.1$ Hz, $B_E = 53.3$ μT and a linewidth of 0.16 Hz, where the contributions from $^{11}BH_4^-$ and $^{10}BH_4^-$ are weighted by 80% and 20%, respectively. As explored in the theory section of this paper, the $^{11}B^1H_4^-$ portion of the spectrum, whose indirect spin–spin coupling constant is 5.2% of the difference in Larmor frequency between ^{1}H and ^{11}B, is well characterized by third-order perturbation theory, with four multiplets whose splittings are strongly dependent on the spin state of the ^{11}B nucleus. T_2 broadening gives the multiplet at 2235 Hz the appearance of a singlet; however the linewidth of this peak is consistent with the splitting of the multiplet predicted by third-order perturbation theory. The contribution from the $^{10}BH_4^-$ anion is a set of seven multiplets, where the central multiplet is largely ob-

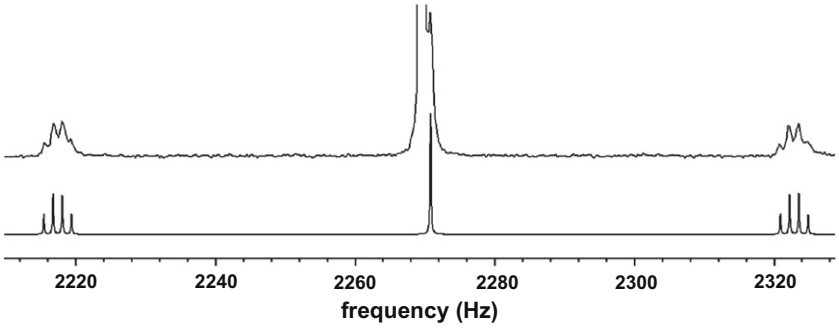

Fig. 3. ^{1}H NMR spectrum of 500 mL 8 M NH_4NO_3 in 2 M HCl. The spectrum was acquired with 49 averages in a total experiment time of 12 min. The central peak at 2269.5 Hz is split into a dominant component which represents the solvent protons and a weaker component, shifted to slightly a higher frequency, which corresponds to the $m = 0$ state of the ^{14}N nucleus. Below the experimental spectrum is a spectrum calculated from second-order perturbation theory using $^1J(^{14}N,^1H) = 52.75$ Hz and $B_E = 53.3$ μT. Very good agreement between the experimental and the calculated spectra is observed.

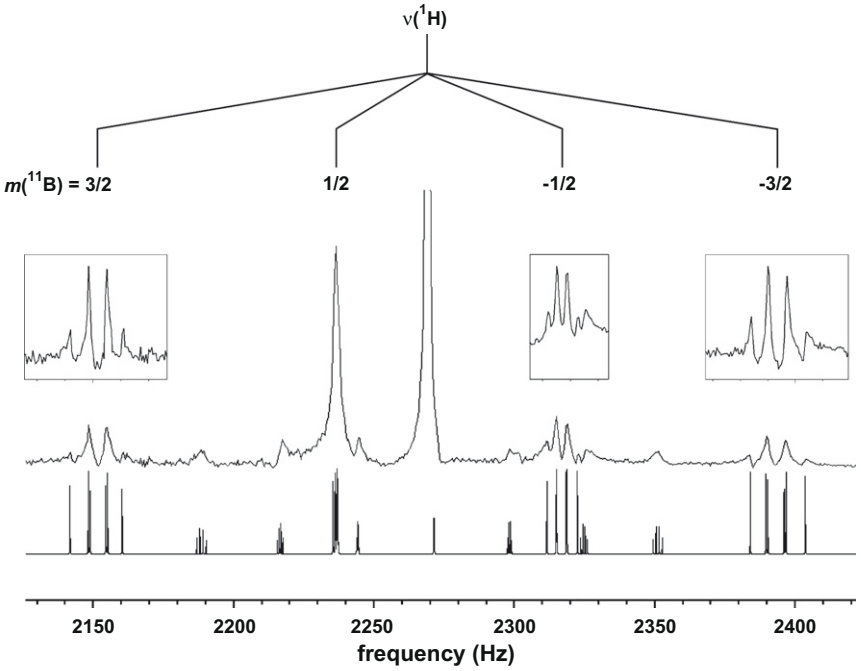

Fig. 4. ^{1}H NMR spectrum of 500 mL 4.5 M $NaBH_4$ in 8 M NaOH. The spectrum was acquired with 4098 averages in a total experiment time of 14 h. Prior to taking the magnitude of the spectrum a complex Lorentzian line centered about 2269.4 Hz with a 1.1 Hz linewidth was subtracted from the experimental spectrum to suppress the dominant peak corresponding to the solvent protons. The central peak in the resultant spectrum is the unsuppressed portion of this solvent proton peak. Below the experimental spectrum is a spectrum calculated from third-order perturbation theory using $^{1}J(^{11}B,^{1}H) = 80.9$ Hz, $^{1}J(^{10}B,^{1}H) = 27.1$ Hz and $B_E = 53.3$ μT, where the contributions from $^{11}BH_4^-$ and $^{10}BH_4^-$ are weighted by 80% and 20%, respectively. A line broadening of 0.16 Hz was added to the calculated spectrum. The insets correspond to three regions of the real spectrum which have been phased locally. Due to imperfections in the transceiver coil a significant phase roll is present over the full spectral width and so the complex spectrum can only be phased locally.

scured by the solvent peak. Under the conditions of this experimental spectrum, $^{1}J(^{10}B,^{1}H)$ is only 1.3% of the difference in Larmor frequency between ^{10}B (243.8 Hz) and ^{1}H (2269.4 Hz) and so it is anticipated that second-order perturbation theory would be sufficient to describe this portion of the spectrum. While the resolution of the experimental spectrum is insufficient to resolve individual peaks within the seven multiplets, the width of these peaks corresponds well with the width of the multiplets calculated using third-order perturbation theory.

4. Conclusions

In this paper we have investigated the unique opportunity presented by high-resolution Earth's field NMR spectroscopy to observe tightly coupled systems of nuclei with differing spin. The utility of second- and third-order perturbation theory for predicting the form of the EFNMR spectra of these tightly coupled systems was demonstrated for the case of protons coupled to ^{14}N ($I = 1$), ^{11}B ($I = 3/2$) and ^{10}B ($I = 3$) nuclei. In addition, we have shown that the use of perturbation theory to describe second- and third-order EFNMR spectra can promote a better understanding of the connection between various spectral features and the underlying quantum mechanical states of the system. We have also noted that Earth's field NMR spectra alone cannot be used to determine the absolute sign of indirect spin–spin coupling constants in systems with only two groups of magnetically equivalent spins, regardless of the spin of the constituent nuclei or the relative strength of the indirect spin–spin coupling between them.

5. Experimental

All experiments were implemented, both at the University of Alberta and Victoria University of Wellington, on a Magritek Terranova-MRI Earth's field system (Magritek Ltd., Wellington, New Zealand) located in a laboratory environment. The pulse sequence used was a simple prepolarize, pulse and collect experiment. Prepolarization was achieved using the standard Terranova-MRI prepolarization electromagnet which provides a field of 18.7 mT at a maximum current of 6 A. Polarization times, on the order of seconds, were chosen to be twice the T_1 of the sample up to a maximum of 6 s. Following an adiabatic switch-off of the prepolarization field, an ultra-low frequency (ULF) excitation pulse was applied for 1.4 ms and the subsequent free-induction decay was recorded. During the multi-scan experiments, temporal variations in the Earth's field were tracked by observing any shifts in the dominant peaks of the ^{1}H EFNMR spectrum. A calibrated B_0 lock coil within the EFNMR probe was used to counter any observed field drift and thus maintain a constant static B_0 field throughout. A 10 mm thick copper box was used as a Faraday shield to screen ultra-low frequency interference. A delay of 300 ms was introduced between the prepolarization pulse and the B_1 excitation pulse in order to avoid any degradation of field homogeneity due to eddy currents induced in the copper box by the switching of the prepolarization field. Details of the experimental apparatus and pulse sequence can be found in [37].

The density matrix simulations and perturbation theory calculations were carried out using the Prospa v2.1 software package (Magritek Ltd., Wellington, New Zealand).

Samples used include: 500 mL of 8 M NH_4NO_3 in 2 M HCl and 500 mL of 4.5 M $NaBH_4$ in 8 M NaOH. All chemicals were purchased from Sigma–Aldrich (USA).

Acknowledgments

M.E.H. and P.T.C. gratefully acknowledge the financial support of the New Zealand Foundation for Research, Science and Technol-

ogy. R.E.W. is a Canada Research Chair in Physical Chemistry at the University of Alberta and thanks the University of Alberta, the Natural Sciences and Engineering Research Council of Canada (NSERC) and the Government of Canada for research support. We also would like to thank Prof. Alex Bain for helpful discussions and Dr. Guy Bernard for helpful comments.

References

[1] M. Packard, R. Varian, Free nuclear induction in the Earth's magnetic field, Phys. Rev. 93 (1954) 941.
[2] G.J. Béné, High resolution NMR spectroscopy in the terrestrial magnetic field range, in: R. Blinc (Ed.), Magnetic Resonance and Relaxation, North-Holland Publishing Company, Amsterdam, 1967, pp. 903–916.
[3] M. Merck, R. Sechehaye, A. Erbeia, G.J. Béné, Free precession experiments in terrestrial magnetic field, in: R. Blinc (Ed.), Magnetic Resonance and Relaxation, North-Holland Publishing Company, Amsterdam, 1967, pp. 952–956.
[4] R.J.S. Brown, B.W. Gamson, Nuclear magnetism logging, Trans. Am. Inst. Mining Metallurg. Petrol. Eng. 219 (1960) 201–209.
[5] D.D. Thompson, R.J.S. Brown, Low-field nuclear magnetic resonance of coupled spin one-half particles, J. Chem. Phys. 35 (1961) 1894.
[6] R.J.S. Brown, D.D. Thompson, Second-order effects in low-field NMR for ammonium ion solutions, J. Chem. Phys. 34 (1961) 1580–1583.
[7] D.D. Thompson, R.J.S. Brown, The Earth's field proton free-precession signal of fluorobenzene, J. Chem. Phys. (1962) 2812.
[8] D.D. Thompson, R.J.S. Brown, Nuclear free precession in very low magnetic fields, J. Chem. Phys. 40 (1964) 3076–3079.
[9] D.D. Thompson, R.J.S. Brown, R.J. Runge, Dynamic nuclear polarization of liquids in very weak fields, Phys. Rev. A Gen. Phys. 136 (1964) 1286–1290.
[10] V.S. Zotev, A.N. Matlashov, P.L. Volegov, I.M. Savukov, M.A. Espy, J.C. Mosher, J.J. Gomez, R.H. Kraus Jr., Microtesla MRI of the human brain combined with MEG, J. Magn. Reson. 194 (2008) 115–120.
[11] S. Xu, C.W. Crawford, S. Rochester, V. Yashchuk, D. Budker, A. Pines, Submillimeter-resolution magnetic resonance imaging at the Earth's magnetic field with an atomic magnetometer, Phys. Rev. A 78 (2008) 013404.
[12] R. McDermott, A.H. Trabesinger, M. Mück, E.L. Hahn, A. Pines, J. Clarke, Liquid-state NMR and scalar couplings in microtesla magnetic fields, Science 295 (2002) 2247–2249.
[13] R. McDermott, N. Kelso, S.K. Lee, M. Mossle, M. Mück, W. Myers, B. ten Haken, H.C. Seton, A.H. Trabesinger, A. Pines, J. Clarke, SQUID-detected magnetic resonance imaging in microtesla magnetic fields, J. Low Temp. Phys. 135 (2004) 793–821.
[14] R. McDermott, S.K. Lee, B. ten Haken, A.H. Trabesinger, A. Pines, J. Clarke, Microtesla MRI with a superconducting quantum interference device, Proc. Natl. Acad. Sci. U. S. A. 101 (2004) 7857–7861.
[15] A.H. Trabesinger, R. McDermott, S.K. Lee, M. Mück, J. Clarke, A. Pines, SQUID-detected liquid state NMR in microtesla fields, J. Phys. Chem. A 108 (2004) 957–963.
[16] S. Appelt, H. Kühn, F.W. Häsing, B. Blümich, Chemical analysis by ultrahigh-resolution nuclear magnetic resonance in the Earth's magnetic field, Nat. Phys. 2 (2006) 105–109.
[17] A. Mohorič, J. Stepišnik, NMR in the Earth's magnetic field, Prog. Nucl. Magn. Reson. Spectrosc. 54 (2009) 166–182.
[18] P.L. Corio, The analysis of nuclear magnetic resonance spectra, Chem. Rev. 60 (1960) 363–429.
[19] W.A. Anderson, Nuclear magnetic resonance spectra of some hydrocarbons, Phys. Rev. 102 (1956) 151–167.
[20] E.W. Garbisch, Analysis of complex NMR spectra for organic chemist. I. Second-order approach with specific application to 2 spin system, J. Chem. Educ. 45 (1968) 311–321.
[21] E.W. Garbisch, Analysis of complex NMR spectra for organic chemist. II. 3 spin systems of ABC ABX ABK and AB2 types, J. Chem. Educ. 45 (1968) 402–416.
[22] E.W. Garbisch, Analysis of complex NMR spectra for organic chemist. III. 4 spin systems of ABC2 ABX2 ABK2 AA'BB' and AA'XX' types, J. Chem. Educ. 45 (1968) 480–493.
[23] P.L. Corio, Structure of High-Resolution NMR Spectra, Academic Press Inc., New York, 1967.
[24] S. Appelt, F.W. Häsing, H. Kühn, J. Perlo, B. Blümich, Mobile high resolution xenon nuclear magnetic resonance spectroscopy in the Earth's magnetic field, Phys. Rev. Lett. 94 (2005) 197602.
[25] H.G. Hecht, Analysis of NMR spectra of magnetically inequivalent nuclei using perturbation theory, Theor. Chim. Acta 3 (1965) 202–210.
[26] C.P. Slichter, Principles of Magnetic Resonance, Springer, Heidelberg, 1990.
[27] L.I. Schiff, Quantum Mechanics, McGraw-Hill, New York, 1968.
[28] P.K. Wang, C.P. Slichter, A pictorial operator formalism for NMR. Coherence phenomena, Bull. Magn. Reson. 8 (1986) 3–16.
[29] O.W. Sørensen, G.W. Eich, M.H. Levitt, G. Bodenhausen, R.R. Ernst, Product operator formalism for the description of NMR pulse experiments, Prog. Nucl. Magn. Reson. Spectrosc. 16 (1983) 163–192.
[30] R.R. Ernst, G. Bodenhausen, A. Wokaun, Principles of Nuclear Magnetic Resonance in One and Two Dimensions, Oxford University Press, Oxford, 1987.
[31] S. Appelt, F.W. Häsing, H. Kühn, U. Sieling, B. Blümich, Analysis of molecular structures by homo- and hetero-nuclear *J*-coupled NMR in ultra-low field, Chem. Phys. Lett. 440 (2007) 308–312.
[32] S. Appelt, F.W. Häsing, H. Kühn, B. Blümich, Phenomena in *J*-coupled nuclear magnetic resonance spectroscopy in low magnetic fields, Phys. Rev. A 76 (2007) 023420.
[33] R.A. Bernheim, B.J. Lavery, Absolute signs of indirect nuclear spin–spin coupling constants, J. Am. Chem. Soc. 89 (1967) 1279–1280.
[34] G.J. Béné, Nuclear magnetism of liquid systems in the Earth field range, Phys. Rep. (Rev. Sect. Phys. Lett.) 58 (1980) 213–267.
[35] R.E. Wasylishen, J.O. Friedrich, Deuterium-isotope effects on the nitrogen chemical-shift and 1*J*(N,H) of the ammonium ion, J. Chem. Phys. 80 (1984) 585–587.
[36] B.E. Smith, B.D. James, R.M. Peachey, Hydrogen-deuterium exchange between MBH_4 and MBD_4 (M = Li, Na) – isotope effects on H-1 and B-11 NMR-spectra of $BHND_4$-*n* anions and a discussion of exchange-reactions in some covalent tetrahydroborate systems, Inorg. Chem. 16 (1977) 2057–2062.
[37] M.E. Halse, A. Coy, R. Dykstra, C.D. Eccles, M.W. Hunter, P.T. Callaghan, Multi-dimensional Earth's field NMR, in: S. Codd, J. Seymour (Eds.), Magnetic Resonance Microscopy, Wiley-VCH, Germany, 2009.